

## Enhanced Malachite Leaching from Jebel Hadieda Region: Surface Dissolution Rate and Response Analysis

Jaber A. Yousif,<sup>1</sup> Ayman M. Ibrahim,<sup>2,3,4, a)</sup> Mohammed Kabashi,<sup>4</sup> Han Wang,<sup>2</sup> and Dianwen Liu<sup>2</sup>

<sup>1)</sup>Department of Mining Engineering, Faculty of Engineering, Eldaein University, Eldaein 63312, Sudan

<sup>2)</sup>State Key Laboratory of Complex Nonferrous Metal Resources Clean Utilization, Kunming University of Science and Technology, Kunming, Yunnan 650093, China

<sup>3)</sup>Department of Mining Engineering, Faculty of Engineering, University of Nyala, Nyala 63311, Sudan

<sup>4)</sup>Department of Mining Engineering, Faculty of Engineering Sciences, Omdurman Islamic University, Khartoum, Sudan

**ABSTRACT:** This study presents a novel approach to enhancing malachite leaching using sulfuric acid ( $H_2SO_4$ ) on ore from the Jebel Hadieda region in South Kordofan State, Sudan, with a copper grade of 7.47%. Microscopic analysis identified the primary copper-bearing mineral, with quartz and clinocllore as the main gangue minerals. The copper mineral's grind size was determined to be 150 microns. The study investigated the effects of several parameters on copper extraction, including particle size, leaching duration, acid concentration, FESEM-EDS, zeta potential, X-ray diffraction, and pulp density. Agitated leaching tests yielded the highest copper extraction (88.15%) at 70 ° C using a  $-212 + 150 \mu m$  particle size, with three hours identified as the optimal leaching duration. Smaller particle sizes provided a greater surface area for acid interaction, accelerating dissolution, while larger particles slowed the dissolution process and reduced copper recovery. These findings indicate that reducing the particle size of malachite to below 300 microns significantly improves leaching efficiency. No previous studies have applied this specific leaching technique for malachite extraction in the Jebel Hadieda region, making this a novel approach.

---

**Received:** 25 Feb. 2025

**Accepted:** 30 April 2025

**DOI:** <https://doi.org/10.71107/wk16ns19>

---

### I. INTRODUCTION

Copper oxide ores are gaining importance as copper sulfide deposits are depleted. Typically found in the weathered zones of primary copper deposits, these ores are generally lower in grade than sulfide ores<sup>1,2</sup>. While they constitute about 20% of total copper reserves, their utilization is increasing due to the depletion of high-grade sulfide ores and advancements in extraction technologies. This growth is driven by the rising use of copper

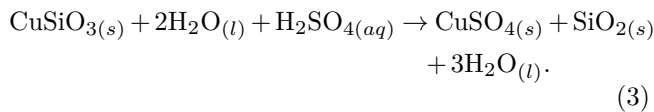
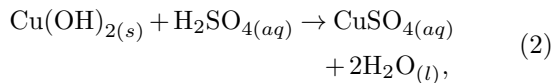
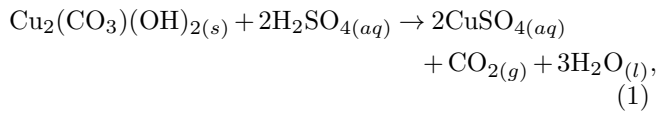
in renewable energy technologies, electric vehicles, and infrastructure development. Consequently, the demand for copper oxide ores is anticipated to grow as they become a more accessible source of copper.

Due to the lower grades of copper oxide ores compared to sulfide ores, hydrometallurgical methods are commonly employed for copper recovery. These methods, such as sulfuric acid leaching, are favored for their effectiveness in extracting copper from these ores<sup>3-6</sup>. Copper extraction relies on different methods depending on the type of ore. Hydrometallurgy is used for oxide ores, while pyrometallurgy is used for sulfide ores<sup>7</sup>. In hydrometallurgical processes, the initial step generally involves leaching<sup>8</sup>. Sudan has a rich and extensive history of gold production, with mining activities dating back to ancient times. It also contains significant porphyry copper-gold mineralization, particularly within the Arabian-Nubian Shield<sup>9</sup>. Despite its valuable mineral resources, the growth of the mining industry has been hindered by political instability, economic sanctions, and inadequate infrastructure, limiting its full po-

---

<sup>a)</sup>Electronic mail: [aymanzrouge@gmail.com](mailto:aymanzrouge@gmail.com)

tential [10]. Due to ongoing conflicts and political instability in that part of Sudan, most of the copper oxide ore in the Jebel Hadieda region was initially extracted by artisanal miners searching for gold<sup>10</sup>. Although the copper oxide content is significant and economically viable, companies have not yet processed it on a large scale. It may become a target ore for future extraction. The Jebel Hadieda area in South Kordofan State, Sudan, is known for its economically viable copper oxide deposits. The study area extends between latitudes (12°N to 13°N) and longitudes (30°E to 31°E), covering an area of about 2.79Km<sup>2</sup> [12]. Geological surveys have identified copper-bearing minerals such as malachite, azurite, cuprite, and chrysocolla in these ores, which are suitable for extraction through hydrometallurgical techniques, particularly sulfuric acid leaching. While copper from sulfide ores is extracted using pyrometallurgical methods, copper from oxide ores is processed using hydrometallurgical methods<sup>11–13</sup>. In pyrometallurgical processes, sulfide ores are treated at high temperatures through smelting and refining to extract copper<sup>14</sup>. In contrast, hydrometallurgical extraction is mainly used for oxide ores, where copper is dissolved using acidic or alkaline solutions during leaching with reagents like HCl, HNO<sub>3</sub>, and H<sub>2</sub>SO<sub>4</sub><sup>8,15–18</sup>. Sulfuric acid leaching is widely used to extract copper from oxide ores because it is cost-effective and efficient. In this process, sulfuric acid reacts with copper oxide minerals to produce soluble copper sulfate, which can then be recovered through solvent extraction and electrowinning (SX-EW) [2123]. The general chemical reactions for this process are provided in eqs. (1) to (3):



Several factors, such as ore mineralogy, particle size, temperature, and acid concentration, significantly affect the efficiency of the leaching process<sup>5,16,19</sup>. In the Jebel Hadieda region, copper oxide ores exhibit variable responses to sulfuric acid leaching, primarily influenced

by the deposits' unique mineralogical and geochemical properties. Studies on copper oxide deposits and sulfuric acid leaching have reported high copper recovery rates under optimal conditions<sup>20,21</sup>. The distinct geological features of Jebel Hadieda ores, such as iron oxides and gangue minerals, require further investigation to assess their potential impact. A comprehensive understanding of this behavior is crucial to optimizing copper extraction and improving the economic viability of mining in South Kordofan.

Although sulfuric acid leaching is widely used for copper oxide extraction, the combined effects of key factors on the leaching of Jebel Hadieda copper oxide ore have not been previously studied. This research investigates how various parameters—including sulfuric acid concentration, leaching time, temperature, and particle size—affect leaching efficiency. Based on ore property research and extensive experiments, leaching processes were conducted under various conditions to determine the optimal leaching index. The work aims to identify the key factors influencing the leaching process to maximize copper recovery while minimizing reagent consumption and operational costs.

## II. MATERIALS AND METHODS

### A. Materials

The copper ore samples were obtained from the region of Jebel Hadieda in South Kordofan State, Sudan, with an estimated probable reserve of 2.5 million tons. The leaching experiments were conducted with analytical-grade sulfuric acid solutions ( 60%H<sub>2</sub>SO<sub>4</sub> ) from Carlo Erba Reagents Co. Ltd. pH regulators and other necessary modifiers were also employed to optimize the leaching conditions.

### B. Sample Preparation

A laboratory jaw crusher reduced the material from 5 cm to 5 mm for sample preparation. The crushed samples were then ground in a laboratory rod mill for 2,5 , and 10 minutes to determine the optimal grinding time. After grinding, sieving was performed to achieve the target particle size of  $-74 + 37\mu$  m. The ore was then divided into two equal portions using riffles of varying sizes. This riffing process was repeated until the required sample size for the experiment was obtained. The sample preparation steps are shown in [Figure 1](#).

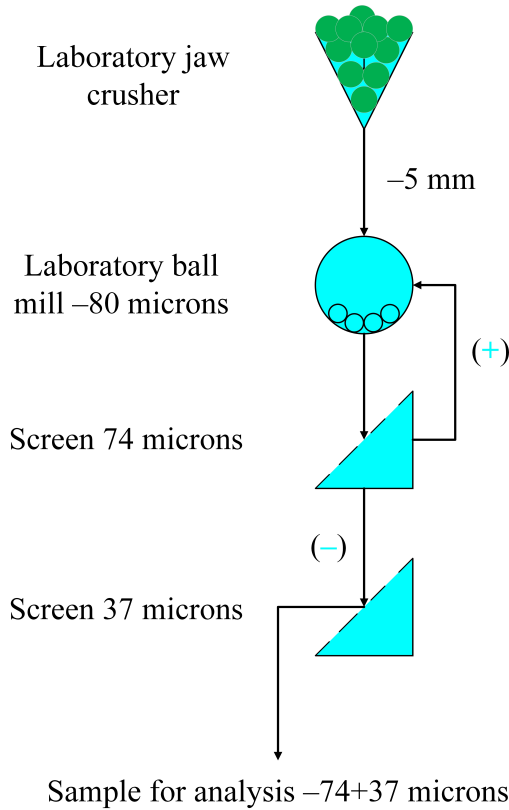


FIG. 1: Sample preparation steps.

**C. Sample Characterization**

A 30 kg representative ore sample containing copper oxide minerals was collected for testing, and the same sample was consistently used throughout the experiments. Chemical and mineralogical characterizations were performed to determine the ore’s general properties. Complete chemical analyses were carried out using atomic absorption spectroscopy (AAS), as shown in [Table I](#).

TABLE I: Chemical analysis results of representative ore samples.

| Components | Cu    | Fe <sub>2</sub> O <sub>3</sub> | SO <sub>4</sub> | SiO <sub>2</sub> |
|------------|-------|--------------------------------|-----------------|------------------|
| Wt. (%)    | 5.105 | 15.68                          | 0.288           | 4.3              |

**D. XRD pattern of pure malachite sample**

The sample was initially crushed to a particle size of -2 mm using jaw and double-roll crushers. A representative portion of the crushed ore was then obtained through the coning and quartering method. Approxi-

mately 70 – 80% of the sample was further crushed to a particle size of minus 160 microns, and it was thoroughly blended and passed through the sets of sieves several times. After sieving, the screen analysis results provided a detailed breakdown of the particle size distribution. The malachite ore sample was ground into a fine powder (approximately -80 microns) to ensure uniformity and optimal diffraction conditions for further chemical analysis. The powder was placed on a sample holder, and X-ray diffraction (XRD) analysis was conducted using a standard diffractometer equipped with a Cu-K  $\alpha$  radiation source ( $\lambda = 1.5406\text{\AA}$ ). The scan covered a  $2\theta$  range of  $10^\circ$  to  $80^\circ$ , with a step size of  $0.02^\circ$  and a counting time of 2 seconds per step. The XRD pattern of the malachite sample is presented in [Figure 2](#).

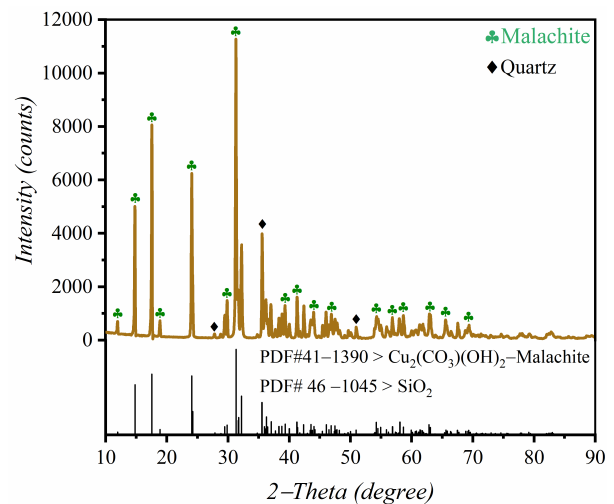


FIG. 2: XRD pattern of pure malachite sample.

**E. Leaching Experimental Approach**

Leaching experiments were conducted using sulfuric acid agitation leaching to optimize copper recovery from copper oxide ore. The representative malachite sample was first ground to -53 microns to increase its surface area and then subjected to batch tests under varying conditions. A sulfuric acid solution of known concentration was prepared and added to the reaction vessel, maintaining a solid-to-liquid ratio of 1:10. The mixtures, with particle sizes ranging from 38 to 45  $\mu\text{m}$ , were stirred continuously to ensure uniform contact between the acid and the ore. The stirring speed was adjusted to a constant 900 rpm. The leaching experiment was conducted at a controlled temperature of  $50^\circ\text{C}$  for 30, 90, and 180 min intervals. Periodic sampling of the leachate was performed to monitor copper dissolution over time.

At the end of the experiment, the leachate was filtered to separate the remaining solid residue from the solution. Copper concentrations in the pregnant leach solution (PLS) were measured using atomic absorption spectroscopy (AAS), and recovery percentages were calculated based on the ore's initial copper content.

#### F. Zeta Potential

Zeta potential measurements were conducted using a Zetasizer analyzer. Fresh sulfuric acid solutions were prepared, and hydrochloric acid (HCl) or sodium hydroxide (NaOH) was added to adjust the pH to a specified value. The effects of various concentrations on the surface charge and stability of malachite in a deionized water background electrolyte solution were observed over a settling period of 5 minutes. The mixture was thoroughly stirred to create a homogeneous suspension, and a sample was then transferred into the Zetasizer cell. The final zeta potential value for the mineral particles was the average of three independent measurements conducted under the same conditions.

#### G. FESEM-EDS Studies

FESEM tests were conducted to investigate the surface morphology of materials at high magnification, utilizing a Nova Nano SEM 450 (FEI, Hillsboro, OR, USA). Energy-dispersive X-ray spectroscopy (EDS) was also used for elemental composition analysis, with an acceleration voltage of 15 kV during detection. The instrument was operated at a 20 kV accelerating voltage and a probe current of 60 mA. Malachite samples weighing 2 g were conditioned with sulfuric acid for 30 minutes. Following solid-liquid separation, the samples were thoroughly washed with deionized water and dried in a vacuum oven. To enhance surface conductivity and prevent interference from electron accumulation, a layer of metal platinum was applied to the samples prior to testing.

### III. RESULTS AND DISCUSSIONS

#### A. Mineralogical analysis

The mineralogical examination of the test sample from the Jebel Hadieda region was conducted under a microscope. This green, copper-bearing mineral was identified as the dominant phase in the sample, underscoring its significance in the ore's copper content.

The microscopic analysis provided detailed insights into the mineral's morphology and distribution, confirming that malachite is the primary source of copper in this deposit. The liberation size (the particle size at which it can be effectively separated from gangue

material during processing) was determined to be 150 microns, as illustrated in Fig. fig. 3(a, b, c, and c). In mineral processing, the liberation size is a critical factor in selecting the appropriate crushing and grinding methods<sup>22-24</sup>. In addition, a liberation size of 150 microns indicates that the material should be ground to this size or smaller to ensure adequate separation of malachite from the gangue, thereby optimizing copper recovery in the subsequent leaching process.

#### B. Screen Analysis

The screen assay analysis of the ore was conducted to assess the distribution of valuable minerals within the sample. The ore was classified into different particle-size fractions, and each fraction was assayed to quantify the concentration of the target minerals. The results of this analysis can be used to inform the development of crushing, grinding, and separation strategies, ultimately optimizing the recovery of valuable minerals during subsequent beneficiation stages<sup>25,26</sup>. Fig. fig. 4 illustrates the dry-screening analysis graph of the composite feed sample and the percent distribution of copper oxide in each fraction. The median size is a critical factor in optimizing processing techniques, as it influences the efficiency of both mineral liberation and subsequent extraction processes<sup>27</sup>. The parameter derived from such curves is the sample's median size, representing the midpoint (or D50) of the particle size distribution, where 50% of the particles are smaller and 50% are larger. This result indicates that the particle size range is likely to dominate processing and recovery and is close to the optimal size for mineral liberation. Table 2 shows no significant differences in copper grades are observed across the various size fractions.

### IV. LEACHING ANALYSIS

#### A. Effect of Leaching Duration and Particle Size

The effect of malachite leaching with sulfuric acid was investigated as a function of both leaching duration (30, 90, and 180 minutes) and particle size ( $-1180 + 600\mu\text{m}$ ,  $-450 + 300\mu\text{m}$ , and  $-212 + 150\mu\text{m}$ ) while maintaining a constant solid-to-liquid ratio (1 : 5 by weight), leaching temperature (room temperature), and sulfuric acid concentration (0.5M, 1M, and 2 M). Both leaching duration and particle size are critical factors influencing the efficiency of copper extraction from malachite ore. The copper extraction values for these tests are provided in Fig. 5. Copper extraction percentages were calculated using the Eq. (IV A) as follows:

$$\text{Extraction (\%)} = 100 - \frac{\text{Cu\% in Residue} \times \text{Wt. of Residue}}{\text{Cu\% in Ore} \times \text{Wt. of Ore}} \times 100$$

TABLE II: Dry Screening Analyses and Mechanical Comminution Results

| Sieve ( $\mu\text{m}$ ) | Size Range     | wt. (g)    | wt.%       | Nominal Aperture ( $\mu\text{m}$ ) | Cum. % Undersize | Cum. % Oversize | Grade % |
|-------------------------|----------------|------------|------------|------------------------------------|------------------|-----------------|---------|
| +2000                   | +2000          | 23.956     | 2.66       | 2000                               | 97.34            | 2.66            | 5.73    |
| -2000 to +1180          | -2000 to +1180 | 63.950     | 7.10       | 1180                               | 90.24            | 9.76            | 6.50    |
| -1180 to +600           | -1180 to +600  | 189.960    | 21.10      | 600                                | 69.14            | 30.86           | 7.11    |
| -600 to +450            | -600 to +450   | 87.956     | 9.77       | 450                                | 59.37            | 40.63           | 5.87    |
| -450 to +300            | -450 to +300   | 70.956     | 7.88       | 300                                | 51.49            | 48.51           | 7.15    |
| -300 to +212            | -300 to +212   | 61.956     | 6.88       | 212                                | 44.61            | 55.39           | 4.99    |
| -212 to +150            | -212 to +150   | 56.198     | 6.24       | 150                                | 38.37            | 61.63           | 5.57    |
| -150 to +100            | -150 to +100   | 63.956     | 7.11       | 100                                | 31.26            | 68.74           | 7.34    |
| -100 to +75             | -100 to +75    | 51.956     | 5.77       | 75                                 | 25.49            | 74.51           | 6.92    |
| -75 to +53              | -75 to +53     | 93.956     | 10.44      | 53                                 | 15.05            | 84.95           | 7.12    |
| -53 (pan)               | -53 (pan)      | 135.200    | 15.05      | -                                  | 0.00             | 100.00          | 8.10    |
| <b>Total</b>            | -              | <b>900</b> | <b>100</b> | -                                  | -                | -               | -       |

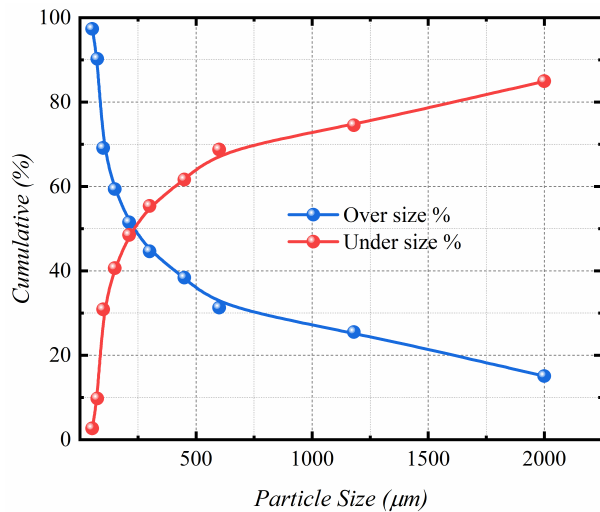


FIG. 3: Dry screening analysis graph

Fig. Figure 4a illustrates the relationship between copper extraction percentage in the leachate and leaching time, revealing a clear trend of increased copper recovery with longer leaching durations. After 30 minutes, copper extraction peaked at approximately 58.49%. With further leaching, the recovery increased to 63.22% after 90 minutes. The maximum copper extraction of 74.56% was achieved after 180 minutes of leaching. Furthermore, the results indicate that the highest copper extraction was achieved with a particle size of approximately 200 microns, where leaching efficiency was significantly greater than larger particles. In contrast, at 600 microns, copper extraction decreased as leaching time increased, likely due to the reduced surface area available for interaction with the leaching solution. Smaller particles ( 200 microns) provide a larger surface area, facilitating better copper dissolution, while larger par-

ticles (600 microns) result in slower and less efficient extraction.

Particle size plays an essential role in the leaching process. Experiments were performed using feed particle sizes of  $-1180 + 600\mu\text{ m}$ ,  $-450 + 300\mu\text{ m}$ , and  $-212 + 150\mu\text{ m}$  to evaluate its effect on copper extraction, as illustrated in Fig. 5b. During these experiments, all other parameters were maintained constant: sample weight ( 50 g ), solid-to-liquid ratio ( 1 : 5 by weight), and  $\text{H}_2\text{SO}_4$  concentration ( 1 M ). Prior to the experiments, it was hypothesized that copper extraction would increase as the ore particle size decreased. This hypothesis was based on the assumption that smaller particle sizes offer a larger interfacial area between the solid particles and the  $\text{H}_2\text{SO}_4$  solution, thereby facilitating a higher transfer rate of copper ions into the solution. Conversely, as particle size increases, the reduced interfacial area is anticipated to hinder the transfer of copper to the leachate.

Contrary to this expectation, the experimental results indicated that particle sizes finer than 300 microns had a marginal effect on copper extraction efficiency. The highest copper extraction was 75%, consistently achieved with the  $-212 + 150\mu\text{ m}$  feed across all leaching durations, with a minimum yield of 38.60% extraction attained within the first 40 minutes. In comparison, larger particle sizes exhibited lower extraction efficiencies: the  $-1180 + 600\mu\text{ m}$  feed yielded a maximum extraction of 69.12% and a minimum of 28.94% at 40 minutes, while the  $-450 + 300\mu\text{ m}$  feed achieved extractions of 31.09% and 63.75% at 40 and 150 minutes, respectively. This trend indicates that coarser particles have a reduced surface area, limiting copper dissolution even with longer leaching times. Overall, the results confirm that copper extraction increases with extended leaching time.

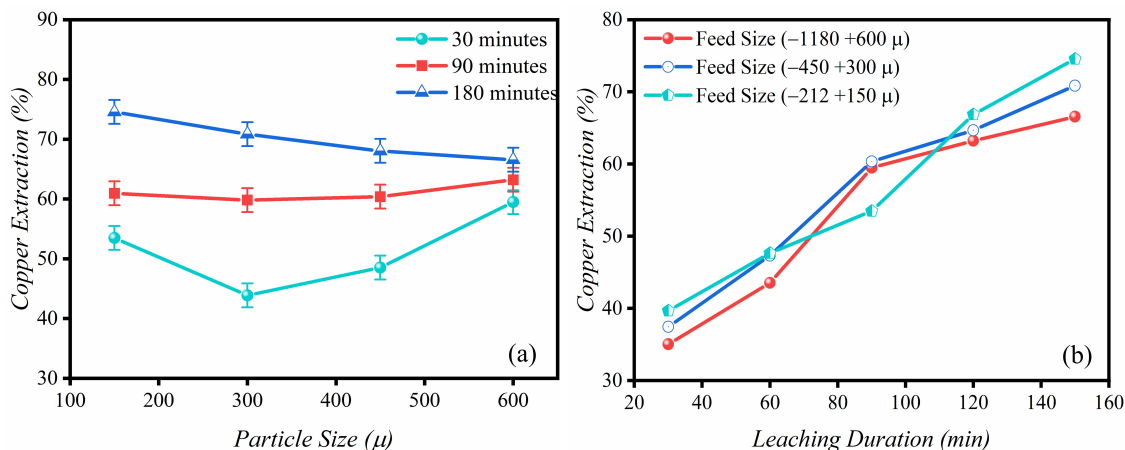


FIG. 4: Copper extraction percentage in the leachate as a function of (a) leaching time and (b) particle size.

### B. Effect of Acid Strength

The effect of acid concentration and leaching time on copper extraction was investigated using three distinct concentrations: 0.5M, 1M, and 2 M. During these tests, conditions such as sample weight (50 g), particle size ( $-212 + 150\mu\text{m}$ ), solid-to-liquid ratio (1 : 5 by weight), and leaching temperature (room temperature) were consistently maintained, as illustrated in Fig. 5a. At 0.5 M acid concentration, copper extraction reached 20.92% after 25 minutes of leaching, increasing to 49.16% after 75 minutes. Beyond 80 minutes, the copper yield stabilized, suggesting that most extractable copper had dissolved, and the transfer rate became negligible. At 1 M acid concentration, copper extraction showed moderate improvement over the 0.5 M results, with increases of 8.64% and 11.36% after 25 and 75 minutes of leaching, respectively. The peak yield was reached at 63.86% after 100 minutes, indicating that a 1 M acid concentration provides more favorable conditions for efficient copper extraction, although the rate of increase slows as saturation approaches. Experiments with a 2 M acid concentration consistently yielded the highest copper extractions across all leaching durations. The elevated sulfuric acid concentration accelerated copper dissolution from the ore, facilitating faster transfer into the leach solution. Copper recovery with  $2\text{MH}_2\text{SO}_4$  showed substantial improvement over the 1 M concentration, particularly after 125 minutes of leaching.

Fig. 5b depicts copper extraction percentages at varying acid concentrations (0.5M, 1M, 2M, and 3 M) across leaching times of 30, 90, and 180 minutes. Each concentration displays a distinct trend, highlighting how copper recovery progresses with extended leaching. The

results indicate a clear pattern: copper extraction yield increases across all leaching durations as acid concentration rises. Higher acid concentrations enhance copper dissolution, speeding its transfer into the leach solution. At 2 M sulfuric acid concentration, copper yields reached 58.14%, 70.23%, and 78.01% after 30, 90, and 180 minutes, respectively. This emphasizes optimizing acid concentration for effective copper recovery throughout the leaching process.

### C. Effect of Temperature

Figure 6 illustrates how temperature, particle size, and sulfuric acid concentration influence copper extraction efficiency in the leachate. Particle size was a key determinant of both the reaction kinetics and overall copper extraction efficiency in the malachite leaching process (Fig. 7a). Smaller particles ( $-212 + 150\mu\text{m}$ ) present a substantially larger surface area, enabling more effective interaction with the leaching agent and achieving the highest copper extraction of 84.5% at  $70^\circ\text{C}$ . This increased surface area accelerates copper dissolution, enhancing the reaction rate and improving extraction efficiency. Medium-sized particles ( $-450 + 300\mu\text{m}$ ) offer a balance between surface area and mass transfer, resulting in a copper extraction of 71.2% at the same temperature. In contrast, larger particles ( $-1180 + 600\mu\text{m}$ ) have a reduced surface area, which slows the reaction kinetics and considerably decreases extraction efficiency, yielding only 50.75% copper extraction under similar conditions. The effect of sulfuric acid concentration on copper extraction from the leachate, using a particle size of ( $-212 + 150\mu\text{m}$ ), as a function of temperature, is shown in Fig. 7b. At

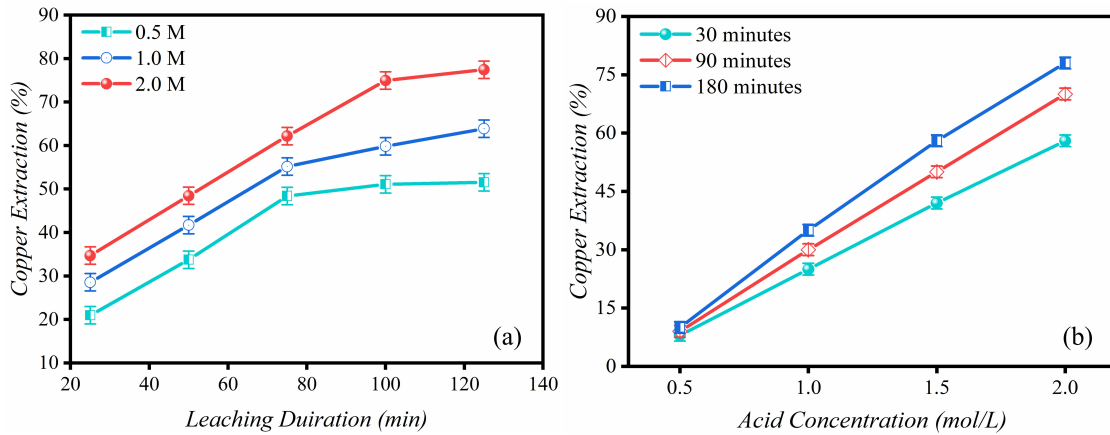


FIG. 5: Copper extraction percentage as a function of (a) sulfuric acid concentration and (b) leaching time.

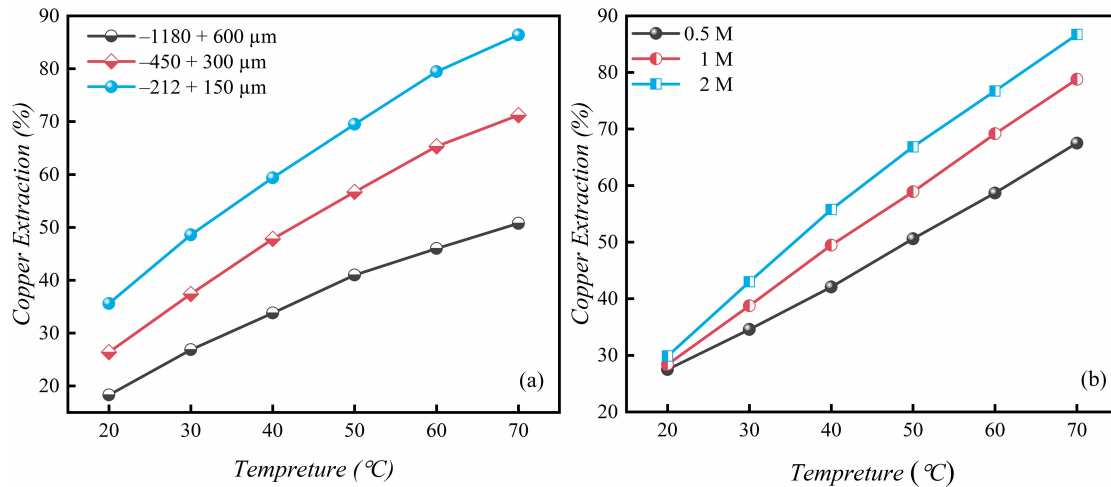


FIG. 6: Effect of temperature on copper extraction as a function of (a) particle size and (b) sulfuric acid concentration.

low acid concentrations ( 0.5 M ), the leaching rate is slower, leading to reduced copper extraction yields. While increasing temperature enhances the dissolution process, the 0.5 M acid concentration remains insufficient to efficiently leach copper, resulting in a maximum extraction of 66.49% at 70°C. The system achieves an optimal balance between acidity and cost at a moderate sulfuric acid concentration (1M). Copper extraction improves with temperature, reaching 78.74% at 70°C, as the acid more effectively breaks down copper-bearing minerals, facilitating faster copper dissolution. At higher acid concentrations ( 2 M ), leaching efficiency improves, yielding higher extraction rates of 88.15% at the same temperature, indicating that elevated temper-

atures lead to superior effectiveness, resulting in better copper recovery compared to lower acid concentrations. Compared to 0.5 M and 1 M acid concentrations, these results show increases in copper extraction yields of 21.66% and 9.41% at the same temperature. This improvement is likely due to the enhanced effectiveness of the leaching process at higher acid concentrations, which enables a more efficient breakdown of copper-bearing minerals.

#### D. Effect of Pulp Density

The effect of pulp density on copper extraction was investigated by testing four different liquidsolid ratios (by weight): 1 : 7, 1 : 6, 1 : 5, and 1 : 4. In these ex-

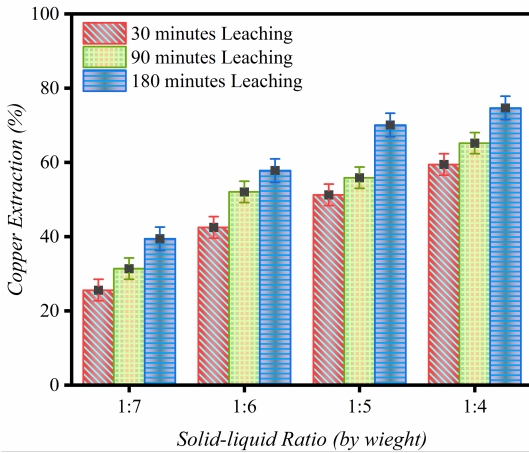


FIG. 7: Effect of liquid-solid ratio on copper extraction as a function of time.

periments, the sample weight ( 50 g ), particle size ( $-1180 + 600\mu m$ ), sulfuric acid concentration (1M), and leaching temperature (room temperature) were kept constant. The results, illustrating the impact of the solid-liquid ratio on copper extraction over time, are presented in Fig. fig. 7.

Initially, the highest copper extraction was observed with a 1 : 7 liquid-solid ratio, yielding a maximum of 39.45% after 180 minutes. This suggests that higher pulp density caused the solid particles to pack more densely, hindering acid penetration and reaction with the ore. In contrast, the 1:6 ratio yielded a slightly higher extraction rate of 57.82%, demonstrating better performance than the 1 : 7 ratio. Furthermore, copper recovery increased to 70.09% with a 1 : 5 liquid-solid ratio. However, the highest extraction rate was achieved with a 4 : 1 ratio, which resulted in a maximum copper yield of 74.7% after 180 minutes. These findings suggest that a lower liquidsolid ratio (higher acid concentration) improves acid dispersion and contact with the malachite particles, ultimately enhancing copper extraction by facilitating more effective acid interaction with the ore’s surface.

### E. Zeta Potential Analysis

Zeta potential measures the repulsion or attraction between particles in a solution, helping assess the stability of colloidal dispersions. It is widely used to examine the relationship between reagent adsorption and the electrokinetic behavior of mineral surfaces<sup>28-31</sup>. Fig. fig. 8 shows the zeta potential of the malachite surface as a function of pH at varying sulfuric acid (  $H_2SO_4$

) concentrations. The isoelectric point (IEP) of pure malachite in a KCl solution is pH 8.7 , which is consistent with previous studies<sup>32-34</sup>. Compared to pure malachite, the zeta potential of the malachite surface in various solution systems exhibits varying degrees of deviation following the addition of sulfuric acid.

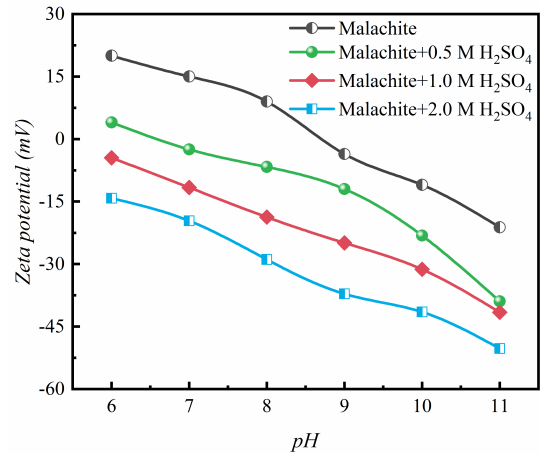


FIG. 8: Zeta potential of malachite as a function of pH under various conditions: (a) pure malachite, (b) 0.5 M  $H_2SO_4$ , (c) 1 M  $H_2SO_4$ , and (d) 2 M  $H_2SO_4$ .

As the pH increases, the potential gradually becomes more negative due to the rising concentration of  $OH^-$  ions and  $CO_3^{2-}$  on the mineral surface, which enhances the electronegativity of anions and results in a more negative malachite surface potential. At pH 9 , the addition of 0.5 M sulfuric acid ( $H_2SO_4$ ) causes the zeta potential of malachite to decrease from -3.63 mV to 12.10 mV . In contrast, with the addition of 1 M and 2M $H_2SO_4$ , a more pronounced negative shift in the surface potential occurs, with the zeta potential decreasing from -24.92 mV to -37.15 mV . These results indicate that higher concentrations of sulfuric acid enhance the dissolution of copper from malachite, thereby improving the leaching process and increasing copper extraction efficiency.

### F. FESEM-EDS Analysis

The FESEM-EDS is used to examine morphological and elemental changes in mineral surfaces, including malachite, and to conduct semi-quantitative analysis with or without different reagents ref40,ref41,ref42,ref43. The malachite ( $Cu_2CO_3(OH)_2$ ) subjected to varying concentrations of sulfuric acid ( $H_2SO_4$ ). The untreated malachite surfaces exhibited a typical smooth, crystalline morphology, with an EDS spectrum revealing an ele-

mental composition of 44.45%Cu, 15.28% C, and 40.27% O. After treatment with 0.5 M sulfuric acid, the surface morphology showed minimal changes, with localized corroded regions. The EDS spectrum indicated an increase in copper (Cu) content to 52.89%, while the atomic concentrations of carbon (C) and oxygen (O) decreased to 12.19% and 34.16%, respectively. Additionally, sulfur (S) was detected at a peak value of 0.10%, suggesting the formation of reaction products such as copper sulfate or other oxidation by-products. More pronounced surface dissolution of malachite was observed at a 1 M concentration of sulfuric acid. The morphology became rougher and more irregular, with distinct white aggregates.

Compared to the previous treatment, EDS analysis showed a significant increase in sulfur and copper contents, reaching 0.24% and 55.21%, respectively, while the atomic concentrations of carbon (C) and oxygen (O) decreased to 17.33% and 27.22%. During the reaction between sulfuric acid and malachite, carbon dioxide (CO<sub>2</sub>) is released, but traces of carbon remain on the surface. Treatment with 2 M sulfuric acid caused extensive dissolution of malachite, with white aggregate dispersions indicating the formation of insoluble copper sulfate (CuSO<sub>4</sub>). Atomic concentration analysis revealed a significant reduction in carbon (17.03%) and oxygen ( 22.76% ) and an increase in sulfur ( 0.60% ) and copper ( 59.61% ). This change is attributed to a disproportionation reaction, in which oxygen from malachite combines with hydrogen ions to form water. The increased sulfur and copper concentrations result from the reaction of sulfuric acid with copper to form copper sulfate, which is soluble in the acidic solution, leading to higher sulfur content in the leachate.

### G. XRD Analysis

X-ray diffraction (XRD) analysis was conducted to examine the changes in the mineralogical composition of malachite after leaching with varying concentrations of sulfuric acid (H<sub>2</sub>SO<sub>4</sub>) (0.5M, 1M, and 2 M ), as shown in Fig. 11. At a 0.5MH<sub>2</sub>SO<sub>4</sub> concentration, the XRD pattern revealed a significant reduction in the intensity of the malachite peaks, indicating partial dissolution (Fig. (Figure 9a)). While the primary malachite peaks remained, their intensity was diminished, suggesting that some copper had been extracted from the mineral structure and copper sulfate (CuSO<sub>4</sub>) formation likely occurred. However, the overall mineral structure remained largely intact under these relatively mild acidic conditions. With the addition of 1MH<sub>2</sub>SO<sub>4</sub>, a further decrease in the intensity of the malachite peaks was observed, indicating a more extensive dissolution

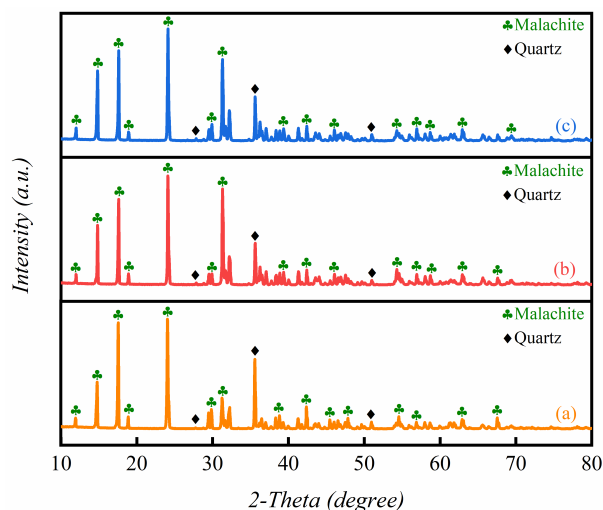


FIG. 9: XRD patterns of malachite leached with different concentrations of H<sub>2</sub>SO<sub>4</sub>: (a) 0.5 M, (b) 1 M, and (c) 2 M.

of the mineral. The XRD pattern showed additional peaks corresponding to copper sulfate ( CuSO<sub>4</sub> ) and possibly other copper-bearing phases (Fig. Figure 9b). Based on the conclusions above, the dissolution rate of malachite in the leachate solution was significantly enhanced by sulfuric acid, facilitating copper extraction and recovery. The ionization and hydrolysis of sulfuric acid (H<sub>2</sub>SO<sub>4</sub>) accelerate the dissolution of malachite by breaking down its mineral structure and releasing copper ions ( Cu<sup>2+</sup> ) into the solution. Sulfuric acid accelerates malachite dissolution by providing hydrogen ions, which react with the malachite and break down its mineral structure<sup>35</sup>. This process occurs at room temperature, although higher temperatures can further enhance the dissolution rate<sup>36</sup>.

The acid components chemically interact with the malachite, releasing copper ions into the solution. This acid-driven reaction produces copper sulfate (CuSO<sub>4</sub>), carbon dioxide (CO<sub>2</sub>), and water (H<sub>2</sub>O). Copper sulfate dissolves in the solution, enabling the extraction of copper, which then dissolves more readily in the leachate. The copper sulfate complexes further promote copper extraction by enhancing dissolution kinetics and improving the overall efficiency of the leaching process, leading to faster and more effective copper recovery.

## V. CONCLUSION

This study investigated optimal conditions for copper recovery from copper oxide ore in the Jebel Hadieda

region of South Kordofan State using agitated sulfuric acid leaching. The main conclusions are as follows:

- The optimal particle size (D50) for mineral liberation was identified. No significant copper grade variation was found across fractions.
- Leaching duration and particle size significantly affect copper extraction. Longer leaching times and smaller particles (200 microns) enhanced recovery, with a maximum yield of 75% after 180 minutes.
- Lower liquid-solid ratios enhance copper extraction. A 1:4 ratio achieved the highest extraction rate (74.7%).
- Temperature, particle size, and sulfuric acid concentration strongly affect extraction efficiency. Smaller particles and higher acid concentrations (2 M) led to a peak yield of 88.15% at 70 °C.
- XRD analysis confirmed that increasing H<sub>2</sub>SO<sub>4</sub> concentration from 0.5 M to 2 M intensified malachite dissolution, leading to higher formation of copper sulfate dissolved in the leachate.

## ACKNOWLEDGMENTS

This research was supported by the National Natural Science Foundation of China (Grant No. 52074138), Yunnan Major Scientific and Technological Projects (Grant No. 202202AG050015), and Basic Research Project of Yunnan Province (Grant No. 202001AS070030 and 202201AU070099).

## DECLARATION OF COMPETING INTEREST

The authors declare that they have no known competing financial interests or personal relationships that could have appeared to influence the work reported in this paper.

## REFERENCES

- <sup>1</sup>M. S. na, E. Gálvez, R. I. Jeldres, *et al.*, “Optimization of Cu and Mn dissolution from black coppers by means of an agglomerate and curing pretreatment,” *Metals* **10**, 657 (2020).
- <sup>2</sup>T. Deng and J. Chen, “Treatment of oxidized copper ores with emphasis on refractory ores,” *Mineral Processing and Extractive Metallurgy Review* **7**, 175–207 (1991).
- <sup>3</sup>A. Neira, D. Pizarro, V. Quezada, and L. Velásquez-Yévenes, “Pretreatment of copper sulphide ores prior to heap leaching: A review,” *Metals* **11**, 1067 (2021).
- <sup>4</sup>B. Xu, Y. Ma, W. Gao, *et al.*, “A review of the comprehensive recovery of valuable elements from copper smelting open-circuit dust and arsenic treatment,” *JOM* **72**, 3860–3875 (2020).
- <sup>5</sup>A. K. Biswas and W. G. Davenport, “Hydrometallurgical copper extraction: Introduction and leaching,” in *Extractive Metallurgy of Copper* (Pergamon, 1980) 2nd ed., pp. 254–270.
- <sup>6</sup>R. Konen and S. Fintov, “Copper and copper alloys: Casting, classification and characteristic microstructures,” in *Copper Alloys – Early Applications and Current Performance – Enhancing Processes* (2012) pp. 3–31.
- <sup>7</sup>K. Rotuska and T. Chmielewski, “Growing role of solvent extraction in copper ores processing,” *Physicochemical Problems of Mineral Processing* **42**, 29–36 (2008).
- <sup>8</sup>H. Kamran Haghighi, D. Moradkhani, B. Sedaghat, *et al.*, “Production of copper cathode from oxidized copper ores by acidic leaching and two-step precipitation followed by electrowinning,” *Hydrometallurgy* **133**, 111–117 (2013).
- <sup>9</sup>F. P. Bierlein, N. Reynolds, D. Arne, *et al.*, “Petrogenesis of a Neoproterozoic magmatic arc hosting porphyry Cu-Au mineralization at Jebel Ohier in the Gebeit Terrane, NE Sudan,” *Ore Geology Reviews* **79**, 133–154 (2016).
- <sup>10</sup>A. Sasmaz, “The Atbara porphyry gold–copper systems in the Red Sea Hills, Neoproterozoic Arabian–Nubian Shield, NE Sudan,” *Journal of Geochemical Exploration* **214**, 106539 (2020).
- <sup>11</sup>W. Yang, Y. Liu, X. Li, *et al.*, “Selective extraction of cobalt and copper from cobalt-rich copper sulfide ores,” *Metallurgical and Materials Transactions B* **54**, 2332–2346 (2023).
- <sup>12</sup>Y. Liao, J. Zhou, F. Huang, and Y. Wang, “Leaching kinetics of calcification roasting calcinate from multimetallic sulfide copper concentrate containing high content of lead and iron,” *Separation and Purification Technology* **149**, 190–196 (2015).
- <sup>13</sup>J. Clark, “The extraction of copper – extracting copper from its ores,” Chemistry LibreTexts (2021).
- <sup>14</sup>R. R. Moskalyk and A. M. Alfantazi, “Review of copper pyrometallurgical practice: Today and tomorrow,” *Minerals Engineering* **16**, 893–919 (2003).
- <sup>15</sup>J. Cao, D. Wu, Q. Zuo, and S. Wen, “Experimental and DFT studies on using Fenton reagent as oxidant to enhance the leaching of cuprite in sulfuric acid system,” *Separation and Purification Technology* **354**, 128693 (2025).
- <sup>16</sup>N. Habbache, N. Alane, S. Djerad, and L. Tifouti, “Leaching of copper oxide with different acid solutions,” *Chemical Engineering Journal* **152**, 503–508 (2009).
- <sup>17</sup>M. D. Sokić, V. D. Milošević, V. D. Stanković, *et al.*, “Acid leaching of oxide–sulfide copper ore prior the flotation – a way for an increased metal recovery,” *Hemijska Industrija* **69**, 453–458 (2015).
- <sup>18</sup>S. Li, Z. Guo, J. Pan, *et al.*, “Stepwise utilization process to recover valuable components from copper slag,” *Minerals* **11**, 211 (2021).
- <sup>19</sup>Q. C. Feng, S. M. Wen, C. Y. Chen, *et al.*, “Extraction of copper from a refractory copper oxide ore by catalytic oxidation acid leaching,” *Advanced Materials Research* **734–737**, 941–944 (2013).
- <sup>20</sup>M. Hosseinzadeh, A. Entezari Zareandi, L. C. Pasquier, and A. Azizi, “Kinetic investigation on leaching of copper from a low-grade copper oxide deposit in sulfuric acid solution,” *Journal of Sustainable Metallurgy* **7**, 1154–1168 (2021).
- <sup>21</sup>S. Khakmardan, A. Shirazi, A. Shirazy, and H. Hosseingholi, “Copper oxide ore leaching ability and cementation behavior, Mesgaran deposit in Iran,” *Open Journal of Geology* **8**, 841–858 (2018).
- <sup>22</sup>P. Semsari Parapari, M. Parian, and J. Rosenkranz, “Breakage process of mineral processing comminution machines – an ap-

- proach to liberation,” *Advanced Powder Technology* **31**, 3669–3685 (2020).
- <sup>23</sup>W. Guo, K. Guo, Y. Xing, and X. Gui, “A comprehensive review on evolution behavior of particle size distribution during fine grinding process for optimized separation purposes,” *Mineral Processing and Extractive Metallurgy Review* **45**, 1–20 (2024).
- <sup>24</sup>K. Chen and W. Yin, “Investigation of liberation properties and mineral fracture mechanisms of iron ores with different mineral grain sizes at different grinding degrees,” *Mineral Processing and Extractive Metallurgy Review* **45**, 397–406 (2024).
- <sup>25</sup>J. J. Frausto, G. R. Ballantyne, K. Runge, *et al.*, “The effect of screen versus cyclone classification on the mineral liberation properties of a polymetallic ore,” *Minerals Engineering* **169**, 106930 (2021).
- <sup>26</sup>W. Zuo, F. Shi, and E. Manlapig, “Pre-concentration of copper ores by high voltage pulses. Part 1: Principle and major findings,” *Minerals Engineering* **79**, 306–314 (2015).
- <sup>27</sup>S. Yenwiset and T. Yenwiset, “Effect of the molten metal stream’s shape on particle size distribution of water atomized metal powder,” *Engineering Journal* **20**, 187–196 (2016).
- <sup>28</sup>R. Liao, S. Wen, Q. Feng, *et al.*, “Activation mechanism of ammonium oxalate with pyrite in the lime system and its response to flotation separation of pyrite from arsenopyrite,” *International Journal of Minerals, Metallurgy and Materials* **30**, 271–282 (2023).
- <sup>29</sup>Y. Fu, W. Yin, X. Dong, *et al.*, “New insights into the flotation responses of brucite and serpentine for different conditioning times: Surface dissolution behavior,” *International Journal of Minerals, Metallurgy and Materials* **28**, 1898–1907 (2021).
- <sup>30</sup>W. Zhao, M. Wang, B. Yang, *et al.*, “Enhanced sulfidization flotation mechanism of smithsonite in the synergistic activation system of copper–ammonium species,” *Minerals Engineering* **187**, 107796 (2022).
- <sup>31</sup>H. Wang, S. Wen, G. Han, and Q. Feng, “Modification of malachite surfaces with lead ions and its contribution to the sulfidization flotation,” *Applied Surface Science* **550**, 149350 (2021).
- <sup>32</sup>G. Liu, Y. Huang, X. Qu, *et al.*, “Understanding the hydrophobic mechanism of 3-hexyl-4-amino-1,2,4-triazole-5-thione to malachite by ToF-SIMS, XPS, FTIR, contact angle, zeta potential and micro-flotation,” *Colloids and Surfaces A: Physicochemical and Engineering Aspects* **503**, 34–42 (2016).
- <sup>33</sup>L. Peng, H. He, Z. Qiu, *et al.*, “Sodium trithiocarbonate as an activator for malachite xanthate flotation: Experimental study and practical application,” *Advanced Powder Technology* **35**, 104426 (2024).
- <sup>34</sup>X. Yu, P. Shen, Z. Yin, *et al.*, “Surface modification of malachite using DMTD and its effect on xanthate adsorption,” *Colloids and Surfaces A: Physicochemical and Engineering Aspects* **679**, 132560 (2023).
- <sup>35</sup>D. Bingöl and M. Canbazoglu, “Dissolution kinetics of malachite in sulphuric acid,” *Hydrometallurgy* **72**, 159–165 (2004).
- <sup>36</sup>O. N. Ata, S. Colak, Z. Ekinici, and M. Copur, “Determination of the optimum conditions for leaching of malachite ore in H<sub>2</sub>SO<sub>4</sub> solutions,” *Chemical Engineering and Technology* **24**, 409–413 (2001).
- <sup>37</sup>C. P. Kujjo, “Mineral exploration and sustainable development: A case study in the republic of South Sudan,” (2019).
- <sup>38</sup>O. Abdelkareem, H. Adam, E. A. Elsiddig, and E. Csaplovics, “Application of remote sensing in the assessment of forest gaps and land use in Umabdalla natural reserved forest, South Kordofan, Sudan,” in *34th Asian Conference on Remote Sensing*, Vol. 4 (2013) pp. 3300–3307.
- <sup>39</sup>J. Sun, T. Zhang, P. Shen, *et al.*, “Kinetics analysis of copper extraction from copper smelting slag by sulfuric acid oxidation leaching,” *Minerals Engineering* **216**, 108886 (2024).
- <sup>40</sup>F. Soltani, H. Darabi, F. Khodabandehlou, *et al.*, “Efficient acid leaching of low carbonate copper oxide ore: A focus on impurity minimization,” *JOM* **76**, 11837 (2024).
- <sup>41</sup>G. M. Pi, “Preparation of copper sulfate solution from copper slag using sulfuric acid solution,” *Advanced Materials Research* **773**, 304–308 (2013).
- <sup>42</sup>J. Yang, Y. Shi, L. Chen, and D. Wu, “Surface oxidation using chlorine dioxide for cuprite and its oxidation leaching mechanism in sulfuric acid solution,” *Applied Surface Science* **637**, 157892 (2023).
- <sup>43</sup>Y. L. Chen, S. R. Wang, J. Ni, *et al.*, “An experimental study of the mechanical properties of granite after high temperature exposure based on mineral characteristics,” *Engineering Geology* **220**, 234–242 (2017).
- <sup>44</sup>Y. Peng, Y. Mao, W. Xia, and Y. Li, “Ultrasonic flotation cleaning of high-ash lignite and its mechanism,” *Fuel* **220**, 558–566 (2018).
- <sup>45</sup>Q. Feng, S. Wen, W. Zhao, *et al.*, “Effect of pH on surface characteristics and flotation of sulfidized cerussite,” *Physicochemical Problems of Mineral Processing* **52**, 676–689 (2016).